Syracuse University

SURFACE

11-12-2005

Inhibition of Cellular Respiration by Doxorubicin

Zhimin Tao
Syracuse University

Henry G. Withers
State University of New York

Harvey S. Penefsky
Public Health Research Institute

Jerry Goodisman
Syracuse University

Abdul Kader Souid
State University of New York

Follow this and additional works at: https://surface.syr.edu/che

Part of the Chemistry Commons

Recommended Citation

Tao, Z., Withers, H. G., Penefsky, H. S., Goodisman, J., & Souid, A. -. (2006). Inhibition of cellular respiration by doxorubicin. Chemical Research in Toxicology, 19(8), 1051-1058.

Inhibition of Cellular Respiration by Doxorubicin

Zhimin Tao,[†] Henry G. Withers,[‡] Harvey S. Penefsky,[§] Jerry Goodisman,*,[†] and
Abdul-Kader Souid*,[‡]

*Department of Chemistry, Syracuse University, CST, 1-014, Syracuse, New York 13244-4100, Department of
Pediatrics, Upstate Medical University, State University of New York, Syracuse, New York 13210-2375, and
Public Health Research Institute, 225 Warren Street, Newark, New Jersey 07103*

Received November 12, 2005

Doxorubicin executes apoptosis, a process known to produce leakage of cytochrome *c* and opening of
the mitochondrial permeability transition pores. To define the loss of mitochondrial function by apoptosis,
we monitored cellular respiration during continuous exposure to doxorubicin. A phosphorescence analyzer
capable of stable measurements over at least 5 h was used to measure $[O_2]$. In solutions containing
glucose and cells, $[O_2]$ declined linearly with time, showing that the kinetics of oxygen consumption
was zero order. Complete inhibition of oxygen consumption by cyanide indicated that oxidations occurred
in the respiratory chain. A decline in the rate of respiration was evident in Jurkat and HL-60 cells exposed
to doxorubicin. The decline was abrupt, occurring after about 2 h of incubation. The inhibition was
concentration-dependent and was completely blocked by the pan-caspase inhibitor benzyloxycarbonyl-
Val-Ala-Asp-fluoromethyl ketone. Respiration in resistant HL-60/MX2 cells, characterized by an altered
topoisomerase II activity, was not inhibited by doxorubicin. A decline in cellular ATP was measured in
Jurkat cells after 2−4 h of incubation with 20 μM doxorubicin, paralleling the decline in respiration rate.
Thus, cells incubated with doxorubicin exhibit caspase-mediated inhibition of oxidative phosphorylation.

Introduction

Doxorubicin, an anthracycline antibiotic, is a widely used
anticancer drug (*1*). This agent intercalates with DNA and
produces DNA breaks by stimulating topoisomerase II-cleavable
complex formation (*2*, *3*). Doxorubicin also targets the mito-
chondria, impairing cellular respiration (*4−7*). In the cell, the
quinone moiety of doxorubicin is reduced to semiquinone
radicals, generating reactive oxygen species, which directly
damage cell organelles (*6*). Oxidative damage produced by the
drug is partially mediated by the doxorubicin−Fe(III) complex
(*8*). The outcome of these events is cell death, primarily by
apoptosis (*9*, *10*).

Apoptosis is executed by a series of cysteine proteases, termed
caspases. Caspase activation leads to mitochondrial dysfunction
(*11*). The mitochondrial perturbation includes opening of the
permeability transition pores (PTP)[1] (*12*). The PTPs, formed at
contact sites between the inner and the outer mitochondrial
membranes, are composed primarily of cyclophilin D (inhibited
by cyclosporine A), the adenine nucleotide translocator (inhib-
ited by bongkrekic acid), and the voltage-dependent anion
channel. The PTPs permit passage of protons (which collapses
the mitochondrial membrane potential, $\Delta\psi$, and leads to
uncoupling of oxidative phosphorylation) and low molecular
weight apoptogenic proteins (e.g., cytochrome *c*, which de-

creases mitochondrial oxygen consumption). It has been sug-
gested that the mitochondrial perturbations are transient (*11*).

Clinically, the maximum concentration of plasma doxorubicin
after 30−60 mg/m^2 iv bolus dosing is 3−10 μM, with $t_{1/2\alpha}$ of
5.0 $\pm$ 2.5 min, $t_{1/2\beta}$ 1.9 $\pm$ 0.6 h, and $t_{1/2\gamma}$ 39 $\pm$ 19 h (*13*).
However, cellular doxorubicin levels are usually 30−100-fold
higher than those of the plasma (*13*). The serious side effects
of doxorubicin that limit its clinical use include cardiomyopathy,
which is, at least partially, a result of drug-induced mitochondrial
impairment (*4*).

Although many of the processes involved in drug-induced
apoptosis have been identified, a full understanding of apoptosis
requires knowledge of the temporal relationships between them.
This necessitates direct measurement of the time course of
individual processes, such as respiration. Here, we measure the
effect of doxorubicin on cellular mitochondrial oxygen con-
sumption during doxorubicin exposure. The rate of respiration
is unchanged for about 2 h, after which it decreases abruptly.
We also measure cellular ATP levels, changes in which parallel
changes in respiration. The results show that cyanide-sensitive
oxidative phosphorylation is inhibited in cells undergoing
apoptosis in response to doxorubicin.

Materials and Methods

Chemicals. Solutions of doxorubicin HCl (3.45 mM) were
purchased from GensiaSicor Pharmaceuticals (Irvine, CA). A
lyophilized powder of caspase inhibitor I (zVAD-fmk, m.w. 467.5)
was purchased from Calbiochem (San Diego, CA). The Pd(II)
complex of *meso*-tetra(4-sulfonatophenyl)tetrabenzoporphyrin (Pd
phosphor sodium salt) was purchased from Porphyrin Products
(Logan, UT). Dulbecco's phosphate-buffered saline (PBS, without
calcium or magnesium), fetal bovine serum, and RPMI-1640
medium (10−040) with L-glutamine (pH 7.15 $\pm$ 0.1) were
purchased from Mediatech (Herndon, VA). Human (promyelocytic)
leukemia (HL-60), HL-60/MX2 (CRL-2257, a mitoxantrone-

---

* To whom correspondence should be addressed. Tel: (J.G.) 315-443-
3035. Fax: 315-443-4070. E-mail: goodisma@mailbox.syr.edu. (A.-K.S.)
Tel: 315-464-5294. Fax: 315-464-7238. E-mail: souida@upstate.edu.
† Syracuse University.
‡ State University of New York.
§ Public Health Research Institute.
[1] Abbreviations: Pd phosphor, palladium derivative of *meso*-tetra(4-
sulfonatophenyl)tetrabenzoporphyrin; *k*, zero-order rate constant for cellular
respiration; zVAD-fmk, benzyloxycarbonyl-val-ala-asp-fluoromethyl ketone;
PTP, permeability transition pores; $\Delta\psi$, mitochondrial electrochemical
potential.

resistant derivative of the HL-60 cell line), and Jurkat clone E6-1 human acute T cell leukemia (TIB-152) cell lines were purchased from American Tissue Culture Collection (Manassas, VA). A luciferin−luciferase mixture (0.2 mg of luciferin and 22000 units of luciferase per vial, stored at −20 °C) and ATP (2 μmol per vial, stored at −20 °C) were purchased from Chrono-Log (Havertown, PA). The remaining reagents were purchased from Sigma-Aldrich (St. Louis, MO).

Solutions. A 2 mM solution of the Pd phosphor was prepared by dissolving the powder at 2.5 mg/mL in dH$_2$O and was stored at −20 °C. Aqueous solutions of ATP (0.4 mM) were prepared in 10 mM Tris-HEPES (pH 7.5) and stored at −70 °C. The final concentration was determined by absorbance at 259 nm using a molar extinction coefficient of 15400 (*14*). A working solution of ATP (4 μM) was prepared fresh in a solution containing 0.1 M Tris-HEPES (pH 7.5), 5 mM MgCl$_2$, and 0.1% fat-free bovine serum albumin. A lyophilized powder containing luciferin (0.2 mg; molecular weight, 280) and luciferase (22000 units) was freshly dissolved in 1.25 mL of PBS, protected from light, and placed on ice. The final concentration of luciferin (570 μM) was determined from its absorbance at 327 nm, using the molar extinction coefficient of 18000 (*14*). NaCN solution was prepared at 2.0 M and brought to pH ∼7.5 with 12 N HCl. The zVAD-fmk solution was made by dissolving 1.0 mg in 1.0 mL of DMSO (final concentration, ∼2.14 mM) and was stored at −20 °C.

Cells. HL-60, the resistant clone HL-60/MX2, and human T-cell lymphoma (Jurkat) cells were maintained in suspension cultures as described (*24*). The resistance of HL-60/MX2 exhibits an altered topoisomerase II catalytic activity and reduced levels of topoisomerase II α and β proteins (*15*). Cell count and viability were determined by light microscopy, using a hemacytometer under standard trypan blue staining conditions.

Incubation with Drugs. Cells were suspended at 10^6 cells/mL in media (containing 6.0 mM Na$_2$HPO$_4$ and 10 mM glucose; pH ∼7.4), 10% fetal bovine serum, 2.0 μM Pd phosphor, and 1% fat-free serum bovine albumin and placed at 37 °C. The drugs (e.g., doxorubicin, zVAD-fmk, and NaCN) were then added. For each condition, 1.0 mL (final volume after all additions, typically <20 μL) of the cell suspension was placed in 1.0 mL glass vials (8 mm clear vials, Krackler Scientific, Albany, NY). The vials were sealed with a crimp top aluminum seal (using a Wheaton hand crimper; Fisher Scientific) and placed in the instrument for oxygen measurements at 37 °C. Mixing was accomplished with the aid of parylene-coated stirring bars (1.67 mm × 2.01 mm × 4.8 mm; V&P Scientific, Inc., San Diego, CA).

Oxygen Consumption. Cellular respiration was measured at 37 °C (*16−19*). The substrate was glucose. The rate of respiration was determined as the negative slope of the curve of [O$_2$] vs t (zero-order rate constant, k, in μM O$_2$ min^{-1} per 10^6 cells). [O$_2$] in the suspension was determined, as a function of time, using the phosphorescence of Pd(II) *meso*-tetra(4-sulfonatophenyl)tetrabenzoporphyrin. The phosphorescence decay of the probe was characterized by a single exponential, with the reciprocal of the phosphorescence decay time (τ) being linear in [O$_2$], according to $\tau^o/\tau = 1 + \tau^o k_q$ [O$_2$]. Here, τ is the lifetime in the presence of oxygen; τ^o is the lifetime in the absence of oxygen; and k_q is the second-order oxygen-quenching rate constant. The drift of the Pd phosphor solution without cells was ≤0.18 μM O$_2$ min^{-1}. zVAD-fmk alone had no effect on the value of k.

Samples were exposed to light flashes (10/s) from a pulsed light-emitting diode array with peak output at 625 nm (OTL630A-5-10-66-E, Opto Technology, Inc., Wheeling, IL). Emitted phosphorescent light was detected by a Hamamatsu photomultiplier tube (#928) after first passing it through a wide-band interference filter centered at 800 nm. The amplified phosphorescence decay was digitized at a rate of 1 MHz by a 20 MHz A/D converter (Computer Boards, Inc.). Two hundred fifty samples were collected from each decay curve, and the data from 10 consecutive decay curves were averaged for calculation of τ. The instrument was calibrated using ascorbate and ascorbate oxidase as described below (*16*).

Phosphorescence measurements on cell suspensions were always carried out simultaneously on 4−6 samples from the same cell culture in order to minimize errors due to variation in culture preparation. Meaningful phosphorescence measurements could not be made until about 30 min after the addition of doxorubicin. This time was required for processing samples, including filling the glass vials, eliminating air bubbles, cleaning and warming the vials to 37 °C, placing them in the instrument, and starting the program. Measurements were then made sequentially on the different samples. The missing points for early times did not affect comparison of the rates of respiration among the different samples of cells from the same culture. Usually, each of the 4−6 samples represented a different condition. The measurements were done simultaneously on these multiple samples from the same culture preparation. Because of variability between culture preparations, it is not meaningful to compare k values obtained with different preparations. Only k values for different conditions using the same preparation are comparable. When duplicate measurements for the same condition and the same preparation were performed, the coefficient of variation in k was less than 10%.

In some measurements, increasing the doxorubicin concentration appeared to be associated with increased values of [O$_2$]. This is believed to be an artifact of the measurement method, associated with the red color of doxorubicin (since the excitation wavelength for the Pd phosphor is 625 nm). The red light scattered by doxorubicin affects the measured phosphorescence decay curve, which is fit to an exponential $Ae^{-t/\tau}$, leading to a lowered value of τ (see equation below) and a higher calculated [O$_2$]. Absorbance measurements in the presence of cells showed that the doxorubicin concentration did not change materially during experiments lasting up to 5 h. Thus, the artifact associated with the red color does not affect the time dependence of [O$_2$].

ATP Content. Acid extracts were prepared by adding 200 μL of 10% perchloric acid to pellets containing 10^6 cells. The mixture was sonicated on ice for 30 s, and the supernatant was collected by centrifugation and neutralized by adding 200 μL of 2.0 M KOH. The sample was incubated on ice for 15 min, and precipitated KClO$_4$ was removed by centrifugation. The ATP content in the resulting supernatant was determined immediately.

The luciferin−luciferase bioluminescence system was used to determine cellular ATP (*14*, *20*). Luminescence was measured at 37 °C using a luminometer (Chrono-Log Corp.) connected to a Chrono-log AGGRO/LINK interface. The data were exported into Microsoft Excel and analyzed as described below. The reaction mixture contained, in a volume of 0.4 mL, 0.1 M Tris-HEPES (pH 7.6), 5 mM MgCl$_2$, 0.1% fat-free bovine serum albumin, and ATP (40−240 pmol) or cellular acid extracts (5−10 μL). The reaction was started by rapidly injecting 10 μL of luciferin/luciferase mixture (5 nmol of luciferin and 176 units of luciferase) from a 50 μL Hamilton syringe into 0.4 mL of rapidly stirred assay mixture.

Light emission was measured every half second for 600 s, and the resulting intensity vs t curve was fit to an exponential, Ae^{-kt}. As shown below, the [ATP] can be obtained from the value of the exponential parameter k. However, [ATP] is proportional to k only for concentrations below ∼0.15 μM; thus, it was necessary to dilute some cellular extracts before the measurements. Furthermore, variations in the luciferin/luciferase used required that each batch be calibrated against standard solutions before use in ATP measurements.

Results

Phosphorescence Calibration. Figure 1A is an example of a titration of dissolved O$_2$ with ascorbic acid in the presence of ascorbate oxidase. Two milliliters of Pd phosphor solution (containing media, 10% fetal bovine serum, 2.0 μM Pd phosphor, 1% fat-free albumin, and 1.25 units of ascorbate oxidase, final pH ∼7.3) was titrated at 37 °C by addition of 10 μL aliquots of 10 mM ascorbate. [O$_2$] was measured electro-
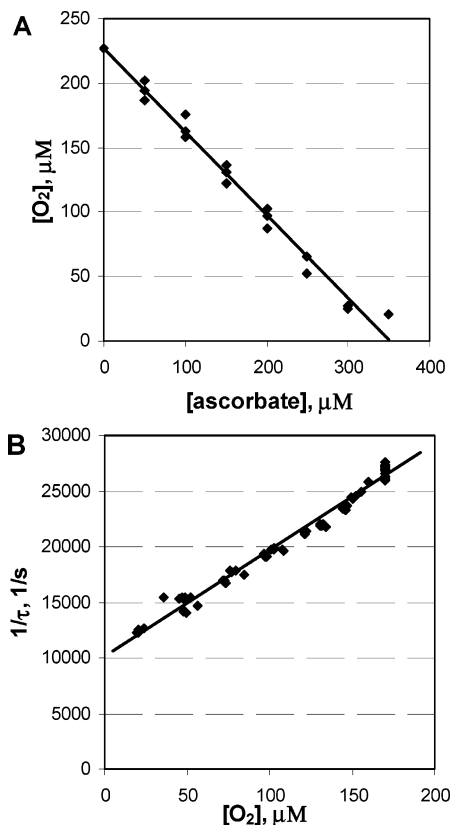
Figure 1. (A) Titration of dissolved O_2 in Pd phosphor solution by ascorbate in the presence of ascorbate oxidase (using the O_2 electrode). Two milliliters of Pd phosphor solution containing media, fetal bovine serum, albumin, and ascorbate oxidase (final pH ∼7.3) was titrated at 37 °C by addition of 10 μL aliquots of 10 mM ascorbate. The apparent stoichiometry (moles of O_2 consumed per moles of ascorbate added) was 0.67 ($r^2 > 0.991$). (B) The reciprocal of measured phosphorescence lifetime ($1/\tau$) is plotted vs electrochemically measured [O_2] in solution (two sets of experiments). The equation $1/\tau = 1/\tau_0 + k_q[O_2]$ is used to convert measured phosphorescence lifetime τ to [O_2]. The quenching constant (k_q), obtained from the slope of the best-fit straight line ($r^2 > 0.92$), is $(152 \pm 11) \times 10^6$ M^{-1} s^{-1}. The value of $1/\tau_0$, from the intercept, is 10087 ± 156 s^{-1}.

chemically, as percent of saturation S. This was converted to molar concentration C according to

$$C = S\frac{0.21 \times (1.013 \times 10^5\,\text{Pa}) \times 55.5\,\text{M}}{100 \times K_H}$$

where $0.21 \times$ (1 atm) is the partial pressure of oxygen in the atmosphere, 55.5 M is the molarity of water, and K_H is the Henry's Law constant for dissolved oxygen in water at 37 °C, 5.211×10^9 Pa. The calculated values of C are plotted in Figure 1A.

[O_2] decreased linearly ($r^2 > 0.991$) with ascorbate added. The slope of the line (−0.668) may be compared with the theoretical stoichiometry (mol of O_2 consumed per mol of ascorbate added) of 0.5. The discrepancy is due to the fact that the total molarity of the solution and the Henry's Law constant used in the equation above are appropriate for pure water, but the values appropriate for our solutions are not known. Multiplication of the above equation by (0.5/0.668) converted percent saturation S, as measured electrochemically, to [O_2] according to $C = S(1.696\ \mu$M).

Phosphorescence lifetimes (τ) were measured in a series of ascorbate/ascorbate oxidase solutions (*16*), simultaneously with electrochemical measurement of [O_2]. Results are shown in
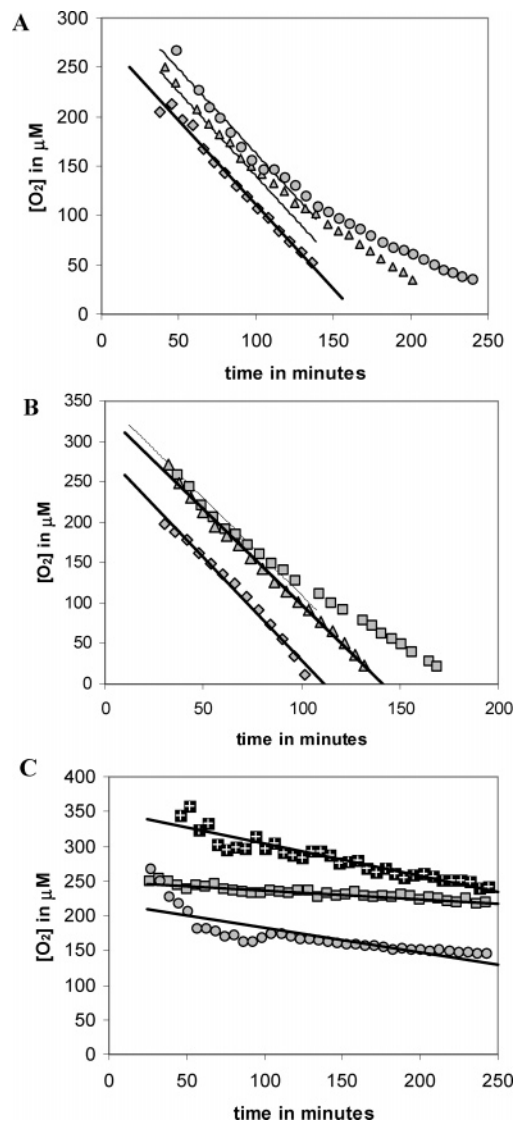

Figure 2. Doxorubicin effect on Jurkat cell respiration. (A) Jurkat cells were suspended at 10^6 cells per mL media, 10% fetal bovine serum, 2 μM Pd phosphor, and 1% albumin. One milliliter of each cell suspension was placed in a 1 mL glass vial, which was sealed and placed in the instrument for [O_2] measurements. Minute zero corresponds to the addition of doxorubicin. Diamonds, untreated cells with best-fit line; triangles and circles, cells treated with 5 and 10 μM doxorubicin, respectively. Lines are drawn parallel to best-fit line for untreated cells. (B) Modulation of doxorubicin effect of cellular respiration by zVAD-fmk. Jurkat cells were processed as above. Minute zero corresponds to the addition of 20 μM doxorubicin. Diamonds, cells plus DMSO with linear fit; squares, cells plus 20 μM doxorubicin plus DMSO with line parallel to previous linear fit; and triangles, cells plus 20 μM doxorubicin plus 20 μM zVAD-fmk with best-fit line. (C) Inhibitory effect of NaCN. Jurkat cells were processed as above. Minute zero corresponds to the addition of 20 μM doxorubicin and 10 mM cyanide. Squares, cells plus 10 mM NaCN with best-fit line (slope = −0.128); circles, cells plus 20 μM doxorubicin with best-fit line after 120 min (slope = −0.20); and filled squares, cells plus 20 μM doxorubicin and 10 mM NaCN with best-fit line (slope = −0.462).

Figure 1B as a plot of $1/\tau$ vs [O_2], which is linear ($r^2 = 0.987$) as it should be according to the theoretical relation:

$$\frac{1}{\tau} = \frac{1}{\tau^o} + k_q[O_2]$$

The value of the quenching constant k_q, determined from the slope of the plot, was $96.1 \pm 1.2\ \mu$M^{-1} s^{-1}. The value of $1/\tau^o$, from the intercept, was (10087 ± 156) s^{-1}. The above equation was used to calculate [O_2] from measured values of τ.
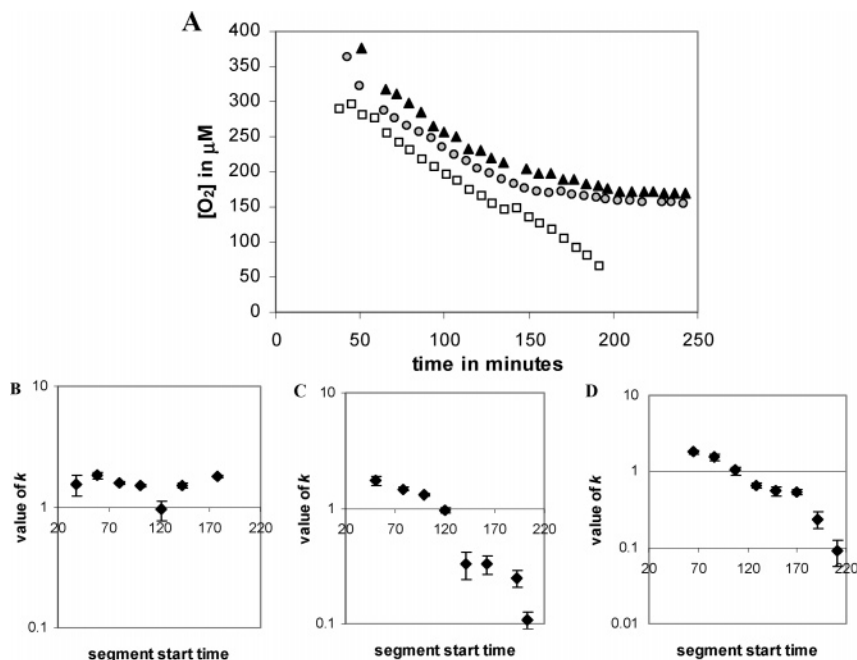
Figure 3. Effects of doxorubicin on the respiration of 10^6 Jurkat cells in 1 mL total volume (sealed). (A) [O_2] as a function of t for untreated cells (empty squares), cells incubated with 20 μM doxorubicin (gray circles), and cells incubated with 40 μM doxorubicin (black triangles). Values of k were derived by fitting six-point segments (corresponding to 35 min) of these plots to lines. (B) Derived k values and statistical errors for no drug, plotted vs segment start time. (C) Derived k values and statistical errors for 20 μM drug, plotted vs segment start time. (D) Derived k values and statistical errors for 40 μM drug, plotted vs segment start time.

Effect of Doxorubicin on Cellular Respiration. Jurkat cell respiration in the presence of 5 and 10 μM doxorubicin is shown in Figure 2A. For untreated cells, respiration was constant and [O_2] was a linear function of time (slope = -1.70 μM O_2/min/10^6 cells). The rate constant k is the negative of the slope. For treated cells, the rate of cellular mitochondrial oxygen consumption was similar to the rate for untreated cells during the first 120 min of drug exposure: $k = 1.71$ μM O_2/min/10^6 cells in the presence of 5 μM doxorubicin and 1.92 μM O_2/min/10^6 cells in the presence of 10 μM doxorubicin. (The dark line in Figure 2A is a least-squares linear fit to the data for untreated cells, and the two fainter lines are drawn parallel to the least-squares fit line.) After 120−140 min, the value of k in the presence of 5 μM doxorubicin declined to 1.23 μM O_2/min/10^6 cells (an approximate 28% decrease from untreated cells), and in the presence of 10 μM doxorubicin, it declined to 0.56 μM O_2/min/10^6 cells (an approximate 67% decrease from untreated cells) (Figure 2A). Similar behavior was observed for cells treated with 20 and 40 μM doxorubicin (data not shown). For $t < 120$ min, [O_2] decreased linearly, with $k = 1.46$ and 1.64 μM O_2/min/10^6 cells, for 20 and 40 μM, respectively. For $t > 140$ min, we found $k = 0.23$ and 0.37 μM O_2/min/10^6 cells, representing 84 and 77% decreases, respectively.

This inhibitory effect of doxorubicin on cellular respiration was completely blocked by the presence of 20 μM of the caspase inhibitor zVAD-fmk (Figure 2B). Three repetitions of these experiments consistently showed very similar results. For the untreated cells in Figure 2B, $k = 2.55$. For the treated cells, $k = 1.49$ for $t > 120$ min (an approximate 42% decrease from untreated cells). With 20 μM zVAD-fmk, the plot of [O_2] vs t was linear for all times, with $k = 2.36$, essentially the same as for untreated cells. Thus, the data show that caspase activities mediate the effect of doxorubicin on mitochondria and that about 2 h is required to execute mitochondrial dysfunction.

The inhibitory effect of NaCN is shown in Figure 2C. The value of k in the presence of 10 mM NaCN was about 0.13 μM O_2/min/10^6 cells. The value of k after 120 min in the presence

of 20 μM doxorubicin was about 0.20 μM O_2/min/10^6 cells. The value of k in the presence of 20 μM doxorubicin plus 10 mM NaCN was about 0.46 μM O_2/min/10^6 cells (Figure 2C). The first two values were similar to the drift observed in the control Pd phosphor solutions (without cells) containing 10 mM NaCN alone (0.10 μM O_2 min^{-1}) or 20 μM doxorubicin (0.29 μM O_2 min^{-1}). Thus, NaCN completely inhibited respiration in treated and untreated cells. Note that k, when both cyanide and doxorubicin were present, was approximately the sum of k in the presence of cyanide and k in the presence of doxorubicin.

Figure 3A shows the analysis of oxygen measurements on 10^6 cells/mL, either untreated or treated with 20 or 40 μM doxorubicin (as in Figure 2). Here, six-point segments (total time 35 min, since measurements were made every 7 min) were fitted to lines; the magnitude of the slope (k) with statistical error is shown in Figure 3B−D, plotted against the start time of the segment. Figure 3B is for no drug, Figure 3C is for 20 μM doxorubicin, and Figure 3D is for 40 μM doxorubicin. In the first case, k was constant, but in the presence of 20 or 40 μM drug, there was a sudden drop in k at about 150 min.

Another way to demonstrate the sudden drop in respiration and also to compare k values for treated and untreated cells for long treatment times involved the following experiment. Two 10 mL cultures of Jurkat cells were prepared; each contained 10^6 cells/mL, one with addition of 20 μM doxorubicin and one without the addition. Both samples were incubated at 37 °C, open to the air. Every hour, starting at $t = 0$, a 1 mL sample of each was taken and placed in sealed vials for phosphorescence measurement of [O_2] in the usual way, alternating between the two. One measurement was made per minute. Because more than 10 min was required to load and equilibrate samples, measurements could be made only ∼15 min after taking a sample. The results are shown in Figure 4A (open circles for no drug and filled squares for 20 μM drug). The set of [O_2] values for each sample was fitted to a line to obtain k. The k values with statistical errors are plotted in Figure 4B. For untreated cells, k was essentially constant, although it increased
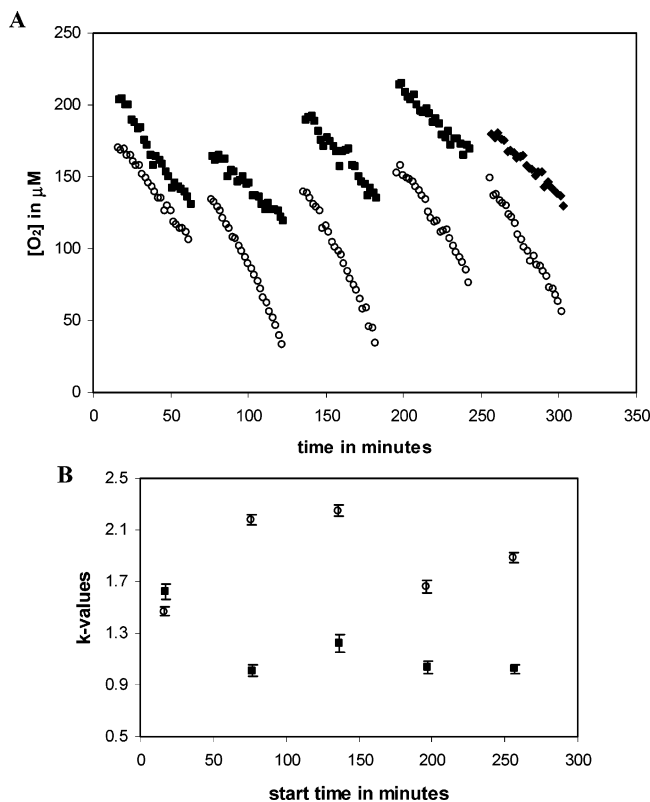
Figure 4. Effect of doxorubicin on the respiration of Jurkat cells. Two cultures of 10^6 cells per mL were incubated at 37 °C, one without drug and one with 20 μM doxorubicin. Every hour, samples of both cultures were withdrawn for measurement of [O_2]. (A) Measured [O_2] vs t. Circles, untreated cells; filled squares, drug-treated cells. (B) Values of k derived from the results of A. For untreated cells, k increased slightly after 1 h and remained constant thereafter; for treated cells, k had the same value as for untreated cells initially but dropped markedly after 1 h and remained constant thereafter.

slightly after the first point (as noted, doxorubicin may increase the rate of respiration at early times). The value of k for treated cells was about the same as for untreated cells at early times (first set of [O_2] values) but dropped after 1 h and remained constant thereafter, never decreasing to zero. Note that, because drug was always present, the incubation time for the second set of [O_2] values was about 100 min. Thus, these experiments show a sudden drop in respiration after about 100 min of incubation. That this is less than previously found times ($\sim$150 min) may be associated with the increased oxygen present.

We next evaluated the respiration of HL-60 cells in the presence of 20 μM doxorubicin, with and without 20 μM zVAD-fmk (Figure 5A). Oxygen consumption was unchanged during the first 150 min of incubation with doxorubicin. The value of k (in μM O_2/min/10^6 cells) for untreated cells was 1.11; for doxorubicin-treated cells ($t < 150$ min), $k = 1.22$; and for doxorubicin-treated cells with 20 μM zVAD-fmk, $k = 1.21$. After 150 min of incubation, the value of k for doxorubicin-treated cells declined to 0.69 (about 43% inhibition). The value of k in the presence of 10 mM NaCN was 0.03 (Figure 5A). Thus, the effect of doxorubicin on HL-60 respiration was very similar to its effect on Jurkat cells.

In HL-60/MX2 cells, the value of k for untreated cells was about 1.65 μM O_2/min/10^6 cells; for cells incubated with 20 μM doxorubicin, the value of k was about 2.94 μM O_2/min/10^6 cells (a 1.8-fold increase); and for cells incubated with 20 μM doxorubicin plus 20 μM zVAD-fmk, the value of k was about 2.87 μM O_2/min/10^6 cells (Figure 5B). These results were consistently reproducible and demonstrated a lack of inhibition
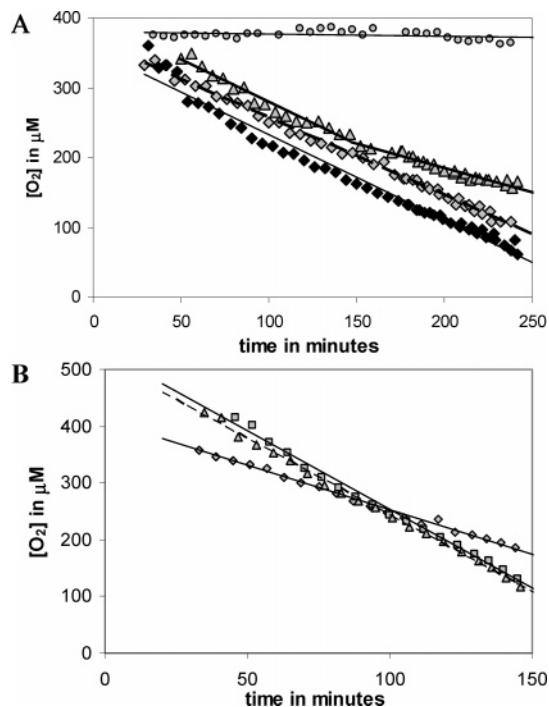

Figure 5. Effects of doxorubicin on the respiration of HL-60 and HL-60/MX2 cells. The cells were processed as described in the legend to Figure 2. Minute zero corresponds to the addition of 20 μM doxorubicin to HL-60 (A) or HL-60/MX2 (B) cells. (A) Solid diamonds, untreated cells with linear fit; triangles, treated cells with fit to two lines for $t <$ 150 min and $t >$ 150 min; light diamonds, treated cells plus 20 μM zVAD-fmk; and circles, cells plus 10 mM NaCN. (B) Diamonds, untreated cells with linear fit; squares, treated cells with linear fit; and triangles, treated cells plus zVAD-fmk.

of respiration in HL-60/MX2 cells during up to 4 h of incubation with 20 μM doxorubicin. The fact that inhibition of respiration by doxorubicin was not observed in HL-60/MX2 cells, which lack topoisomerase II activity, indicated that topoisomerase II was required for doxorubicin-induced execution of apoptosis and promotion of mitochondrial dysfunction. It also appears that doxorubicin enhanced HL-60/MX2 respiration $\sim$1.8-fold. This drug effect was fully inhibited by cyanide or rotenone (not shown). Thus, the enhancement was not mediated by redox cycling of doxorubicin by mitochondria (*6*).

Luminescence Calibration. Cellular ATP was determined from the luminescence vs time curve in the presence of luciferin and luciferase. The observed luminescence as a function of time should follow $\alpha e^{-\gamma t} + \beta$, with α proportional to the initial [ATP]. Attempts to fit our experimental data to this three-parameter form were unsuccessful because the scatter in measured intensities was a large fraction of the variation in light intensity over 600 s, making the determination of three parameters unreliable. (Typical intensity plots are shown in the top panel of Figure 6.) Instead, we fit our data to the two-parameter exponential form Ae^{-kt}, as shown in the top panel of Figure 6, for which the exponential fits are $41.27\ e^{-0.00035t}$ and $35.43\ e^{-0.00042t}$. It is obvious that, if α is much smaller than β (very small [ATP]), k will approach 0, whereas if α is much larger than β (very large [ATP]), k will approach γ, the rate constant for the ATP−luciferin reaction. For small [ATP], the value of k must be proportional to α/β, i.e., to the initial [ATP]; but for larger [ATP], the value of k will approach a limiting value.

This behavior is shown in the bottom panel of Figure 6, which gives the results (k values) of fitting exponentials to luminescence vs time data sets obtained for a series of solutions of
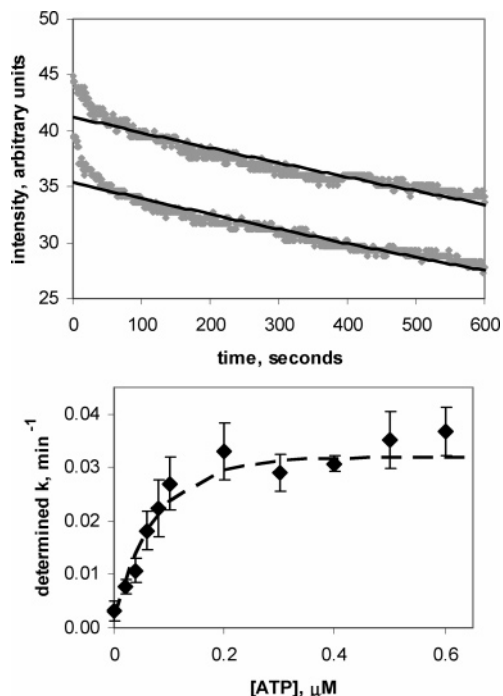
Figure 6. Top panel: Plots of measured luminescence intensity L vs *t*, with exponential fits [$L = A \exp(-kt)$], from which *k* values and [ATP] are determined (see below). These results are for [ATP] = 0.10 μM. The best-fit exponentials, shown, are 41.27 $e^{-0.00035t}$ and 35.43 $e^{-0.00042t}$. Bottom panel: Calibration curve for luminescence measurement of ATP. Three solutions were prepared for each ATP concentration indicated. Luminescence intensity as a function of time was measured for each solution out to 600 s and fitted to the exponential [$A \exp(-kt)$]. Average values of *k* and standard deviations are shown for each concentration. The value of *k* is linear in [ATP] for [ATP] < 0.15 μM (the dashed curve is a fit to $k = b\{1 - \exp(-c[\text{ATP}])\}$); so, for accurate determination of ATP, some solutions were diluted before measurement.

known [ATP] from 0 to 0.6 μM. Three data sets were obtained and analyzed for each [ATP]. In the bottom panel of Figure 6, we plot the average value of *k* with the standard deviation. (The dashed curve is a fit to the analytic form, $k = a - be^{-c[\text{ATP}]}$, for clarity.) It is evident that one can measure [ATP] reliably by our method only when [ATP] is less than 0.2 μM. For solutions of higher [ATP], it was required to dilute the sample before measurement to make [ATP] less than 0.2 μM. It should be noted that the calibration against standard ATP solutions has to be performed for each luciferin solution, because of variations from one preparation to another, and the experimental measurements should be done soon after calibration, because the solution degrades in a few days.

Cellular ATP. Jurkat cells were suspended at 10^6 cells per mL media with 10% fetal bovine serum and 1% albumin and incubated at 37 °C in sealed containers for up to 3 h. The results of measurement of ATP are shown in Figure 7, as 100 times the ratio of measured ATP at time *t* to measured ATP at time 0. Three conditions were used as follows: no addition of drug (circles), with addition of 20 μM doxorubicin (squares), and with addition of 20 mM NaCN (triangles). At 1 h intervals after addition of doxorubicin or cyanide, three 1 mL samples of each cell suspension were taken for analysis of ATP. With no addition, cellular ATP remained constant. The addition of doxorubicin had no effect on cellular ATP at 1 h, but at 3 h, ATP decreased to 36% of its initial value. The addition of cyanide produced a sharp decrease in cellular ATP at 1 h and a further decrease to 20% of its initial value at 3 h. For all three conditions, there was a small increase in cellular ATP between
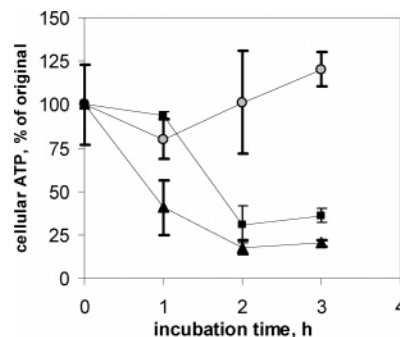

Figure 7. Effect of doxorubicin on cellular ATP. Jurkat cells were suspended at 10^6 cells per mL media, with 10% fetal bovine serum and 1% albumin, and incubated at 37 °C in sealed containers either alone (open circles), with 20 μM doxorubicin (squares), or with 20 mM NaCN (triangles). At indicated time points ($t = 0$ corresponds to the addition of doxorubicin or NaCN), three 1 mL samples of each cell suspension were removed and processed for cellular ATP determination. ATP concentrations are given as percents of concentration at $t = 0$ (before incubation). Mean and standard deviations are shown for each measurement.
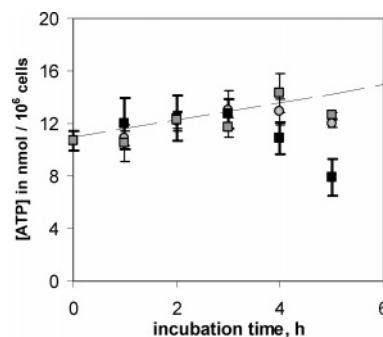

Figure 8. Jurkat cells were suspended at 10^6 cells per mL media with 10% fetal bovine serum and 1% albumin and incubated at 37 °C with stirring in containers open to the air. Under these conditions of incubation, stirring reintroduced oxygen into the suspension so the [O_2] of the cell suspension did not decrease with *t*. The reaction mixtures contained no additions (circles), 20 μM doxorubicin (dark squares), or 20 μM doxorubicin plus 20 μM zVAD (light squares). At 1 h time intervals, three samples of each condition were analyzed for ATP as described. Mean [ATP], with standard deviations, is shown. The dashed line is a linear fit to the first four points, showing that doxorubicin treatment did not decrease cellular ATP during the first 3 h.

2 and 3 h; further investigation will be necessary to determine whether this increase is significant.

A second series of experiments was designed to show the effect of zVAD. Jurkat cells were suspended at 10^6 cells per mL media with 10% fetal bovine serum and 1% albumin and incubated at 37 °C in containers open to the air for up to 5 h (Figure 8). Three conditions were used as follows: untreated (circles), addition of 20 μM doxorubicin (dark squares) and addition of 20 μM doxorubicin plus 20 μM zVAD (light squares). At time 0 and at five succeeding 1 h time intervals, three samples were collected from each of the three conditions and analyzed for ATP as described above. Each result shown in Figure 8 is the mean of three values with standard deviations. For untreated cells, ATP did not decrease during the 5 h period and may even have increased (slope = 0.38 ± 0.18 nmol/10^6 cells/h). With 20 μM doxorubicin, there was an overall decrease of about 25% in cellular ATP. However, there was no apparent effect for the first 3 h: The slope of the line fitted to the first four points, shown as a dashed line in Figure 8, was actually positive (0.66 ± 0.16 nmol/10^6 cells/h). After 3 h, cellular ATP decreased rapidly (the slope of the linear fit to the last three points was −2.4 ± 0.3 nmol/10^6 cells/h). With 20 μM zVAD

added in addition to 20 μM doxorubicin, cellular ATP did not decrease with time. Indeed, cellular ATP increased slightly: The slope was 0.59 ± 0.24 nmol/10^6 cells/h, equal (within statistical error) to the slope for untreated cells and to the slope for doxorubicin-treated cells for $t \leq 3$ h. It is clear that zVAD nullifies the doxorubicin-induced attenuation of cellular ATP as well as the doxorubicin-induced inhibition of respiration.

Discussion

Anthracyclines are known to target the mitochondria ([4–7]). However, incubations of beef heart submitochondrial particles with doxorubicin produced no noticeable effect on oxygen consumption ([17]). Thus, the effect of this drug on cellular respiration is likely indirect, perhaps mediated by induction of apoptosis. We utilized zVAD-fmk (a pan-caspase family inhibitor) ([21]) in order to investigate whether caspases mediate doxorubicin's effect on cellular respiration (Figures 2B and 5). Resistant (HL-60/MX2) and sensitive (HL-60 and Jurkat) cells were used to explore the role of topoisomerase II activity (deficient in HL-60/MX2) in doxorubicin-induced mitochondrial dysfunction. Cellular oxygen consumption (Figures 2–5) and ATP content (Figures 7 and 8) were determined during continuous exposure to doxorubicin. The presence of cyanide in these experiments inhibited cellular respiration (Figures 2C and 5A) and ATP content (Figure 8), thus establishing that both processes occurred primarily in association with oxidations in the respiratory chain.

The results show that doxorubicin induces apoptosis (activation of caspases), which impairs respiration. Thus, the decrease in oxygen consumption is a consequence of apoptosis. The fact that the combination of cyanide and doxorubicin leads to greater oxygen consumption than with cyanide alone (Figure 2C) suggests that doxorubicin may slightly stimulate oxygen consumption, as shown previously ([4, 5]).

It has been reported that doxorubicin increased the permeability of the inner mitochondrial membrane by opening the mitochondrial PTP. In adenocarcinoma cells, doxorubicin (17 μM for 60 min) decreased the value of $\Delta\psi$ by about 30%, an effect that was blocked by zVAD-fmk ([7]). Such an effect on $\Delta\psi$ would be expected to uncouple phosphorylation from oxidation. In addition, doxorubicin increases the permeability of the outer mitochondrial membrane to cytochrome c, an effect that is expected to decrease mitochondrial respiration.

The inhibitory effect of doxorubicin on respiration, observed in our experiments on Jurkat and HL-60 cells, was evident within 2–3 h of incubation with the drug (Figures 2A,B and 5A). This inhibitory effect was blocked by zVAD-fmk (Figures 2B and 5A) and was not observed in HL-60/MX2 cells (Figure 5B), which lacked topoisomerase II activity. Thus, it is clear from these observations that doxorubicin-induced inhibition of respiration requires caspase and topoisomerase II activities.

The rate of respiration in cells exposed to the drug remains close to the rate in untreated cells for about 2.5 h and then decreases, remaining relatively constant thereafter. (For cells exposed to the drug in the presence of air, the decrease in k occurs sooner, at about 1.5 h, as seen in Figure 4. It is known that drugs such as doxorubicin are more effective in inducing apoptosis when oxygen is present, possibly because reactive oxygen species play a role.) As will be shown in a future publication, other apoptosis-inducing drugs (e.g., actinomycin D) behave differently: They decrease respiration in Jurkat cells gradually, starting at the earliest times for which measurements can be made. The data in Figure 7 show that ATP levels do not

decrease for at least 1 h of the treatment, and a significant decrease has occurred by 2 h, slightly earlier than for respiration.

Observations relevant to the role of mitochondrial $\Delta\psi$ were presented in a series of papers by Green and co-workers ([22–24]) who examined the apoptotic response of HL-60 and other cells following short exposures to actinomycin D, etoposide, or staurosporine. It was found that apoptosis was initiated without significant changes in $\Delta\psi$ and the changes in $\Delta\psi$ occurred only later in the cell death pathway. The authors concluded that collapse of $\Delta\psi$, resulting from formation of the PTP, was not a critical feature of apoptosis ([22]). Studies of single cells treated with etoposide or actinomycin D showed that, if caspases were not activated, the mitochondria maintained critical functions, such as the generation of ATP, even after release of cytochrome c ([23]). In contrast, caspase activation disrupts complexes I–II of the mitochondrial electron transport chain, resulting in diminished $\Delta\psi$ and generation of reactive oxygen species ([24]). The results in Figures 2 and 3 and Figures 7 and 8 agree with these reports and show that caspase activation impairs oxidative phosphorylation. The decrease in cellular ATP (Figures 7 and 8) also emphasizes the importance of mitochondrial death during apoptosis ([11]).

Mizutani et al. ([25]) found that incubation of HL-60 cells with doxorubicin for up to 8 h led to H_2O_2-mediated oxidative damage of DNA, which in turn led to an indirect generation of H_2O_2 via activation of NAD(P)H oxidase. The end result was an increase in $\Delta\psi$ and activation of caspase-3. Doroshow ([4]) reported that high concentrations of doxorubicin (135 μM) stimulated oxygen consumption when added to isolated cardiac mitochondria. The stimulation was more readily demonstrable in the presence of KCN and rotenone. The overall increase in oxygen consumption was attributed to the production of superoxide anion ([5]). The enhancement of O_2 consumption was immediate, required NADH, and was more pronounced in the presence of rotenone or cyanide. It was concluded that mitochondrial NADH dehydrogenase reduced doxorubicin to its semiquinone, with subsequent transfer of electrons to O_2 ([5–7]).

The observation that oxygen consumption in the present experiments was completely inhibited by NaCN (Figures 2C and 5A) strongly supports the conclusion that the observed O_2 consumption occurred in the mitochondrial respiratory chain. If reactive oxygen species were produced, their amounts did not significantly add to the observed respiration. It is also unlikely that small amounts of reactive oxygen intermediates were responsible for the observed inhibition of respiration and lowering of ATP levels since the effects of doxorubicin were prevented when zVAD-fmk was included in incubation mixtures. Thus, it is clear that, in our experiments, doxorubicin treatment executed apoptosis within about 2 h of drug exposure, decreasing mitochondrial oxidative phosphorylation (Figures 2–4 and 8). Furthermore, the decline in cellular ATP contributed to the mechanism of cell death by apoptosis (Figures 7 and 8). It is worth noting that the doxorubicin-induced cellular ATP depletion started earlier and was more pronounced in the sealed vials (Figure 7) than the open containers (Figure 8).

In summary, the results presented show that cells exposed to doxorubicin exhibit partial, dose-dependent inhibition of oxidative phosphorylation. The inhibition occurs after a few hours of exposure to the drug, is mediated by caspases, and requires topoisomerase II activity.

References

(1) Binaschi, M., Bigioni, M., Cipollone, A., Rossi, C., Goso, C., Maggi, C. A., Capranico, G., and Animati, F. (2001) Anthracyclines: Selected new developments. *Curr. Med. Chem. 1*, 113−130.

(2) Zunino, F., and Capranico, G. (1990) DNA topoisomerase II as the primary target of antitumor anthracyclines. *Anticancer Drug Des. 5*, 307−317.

(3) Nitiss, J. L. (2002) DNA topoisomerases in cancer chemotherapy: Using enzymes to generate selective DNA damage. *Curr. Opin. Invest. Drugs 3*, 1512−1516.

(4) Doroshow, J. H. (1983) Effect of anthracyclines antibiotics on oxygen radical formation in rat heart. *Cancer Res. 43*, 460−472.

(5) Davis, K. J., and Doroshow, J. H. (1986) Redox cycling of anthracyclines by cardiac mitochondria. I. Anthracycline radical formation by NADH dehydrogenase. *J. Biol. Chem. 261*, 3060−3067.

(6) Doroshow, J. H., and Davis, K. J. (1986) Redox cycling of anthracyclines by cardiac mitochondria. II. Formation of superoxide anion, hydrogen peroxide and hydroxyl radical. *J. Biol. Chem. 261*, 3068−3074.

(7) Huigsloot, M., Tijdens, I. B., Mulder, G. J., and van de Water, B. (2002) Differential regulation of doxorubicin-induced mitochondrial dysfunction and apoptosis by Bcl-2 in mammary adenocarcinoma (MTLn3) cells. *J. Biol. Chem. 277*, 35869−35879.

(8) Kostoryz, E. L., and Yourtee, D. M. (2001) Oxidative mutagenesis of doxorubicin-Fe(III) complex. *Mutat. Res. 490*, 131−139.

(9) Bellarosa, D., Ciucci, A., Bullo, A., Nardelli, F., Manzini, S., Maggi, C. A., and Goso, C. (2001) Apoptotic events in a human ovarian cancer cell line exposed to anthracyclines. *J. Pharmacol. Exp. Ther. 296*, 276−283.

(10) Lorenzo, E., Ruiz-Ruiz, C., Quesada, A. J., Hernandez, G., Rodriguez, A., Lopez-Rivas, A., and Redondo, J. M. (2002) Doxorubicin induces apoptosis and CD95 gene expression in human primary endothelial cells through a p53-dependent mechanism. *J. Biol. Chem. 277*, 10883−10892.

(11) Green, D. R., and Kroemer, G. (2004) The pathophysiology of mitochondrial cell death. *Science 305*, 626−629.

(12) Batandier, C., Leverve, X., and Fontainer, E. (2004) Opening of the mitochondrial permeability transition pore induces reactive oxygen species production at the level of the respiratory chain complex I. *J. Biol. Chem. 279*, 17197−17204.

(13) Speth, P. A., Linssen, P. C., Boezeman, J. B., Wessels, H. M., and Haanen, C. (1987) Cellular and plasma adriamycin concentrations in long-term infusion therapy of leukemia patients. *Cancer Chemother. Pharmacol. 20*, 305−310.

(14) Lemasters, J. J., and Hackenbrock, C. R. (1979) Continuous measurements of adenosine triphosphate with firefly luciferase luminescence. *Methods Enzymol. 56*, 530−544.

(15) Harker, W. G., Slade, D. L., Drake, F. H., and Parr, R. L. (1991) Mitoxantrone resistance in HL-60 leukemia cells: Reduced nuclear topoisomerase II catalytic activity and drug-induced DNA cleavage in association with reduced expression of the topoisomerase II β isoform. *Biochemistry 30*, 9953−9961.

(16) Lo, L.-W., Koch, C. J., and Wilson, D. F. (1996) Calibration of oxygen-dependent quenching of the phosphorescence of Pd-meso-tetra (4-carboxyphenyl) porphine: A phosphor with general application for measuring oxygen concentration in biological systems. *Anal. Biochem. 236*, 153−160.

(17) Souid, A.-K., Tacka, K. A., Galvan, K. A., and Penefsky, H. S. (2003) Immediate effects of anticancer drugs on mitochondrial oxygen consumption. *Biochem. Pharmacol. 66*, 977−987.

(18) Tacka, K. A., Dabrowiak, J. C., Goodisman, J., Penefsky, H. S., and Souid, A.-K. (2004) Quantitative studies on cisplatin-induced cell death. *Chem. Res. Toxicol. 17*, 1102−1111.

(19) Tacka, K. A., Szalda, D., Souid, A.-K., Goodisman, J., Dabrowiak, J. C. (2004) Experimental and theoretical studies on the pharmacodynamics of cisplatin in Jurkat cells. *Chem. Res. Toxicol. 17*, 1434−1444.

(20) Karamohamed, S., and Guidotti, G. (2001) Bioluminometric method for real-time detection of ATPase activity. *BioTechniques 31*, 420−425.

(21) Slee, E. A., Zhu, H., Chow, S. C., MacFarlane, M., Nicholson, D. W., and Cohen, G. M. (1996) Benzylooxycarbonyl-Val-Ala-Asp (Ome) fluormethyl ketone (Z-VAD.FMK) inhibits apoptosis by blocking the processing of CPP32. *Biochem. J. 315*, 21−24.

(22) Finucane, D. M., Waterhouse, N. J., Amarante-Mendes, G. P., Cotter, T. G., and Green, D. R. (1999) Collapse of inner mitochondrial transmembrane potential is not required for apoptosis of HL60 cells. *Exp. Cell Res. 251*, 166−174.

(23) Waterhouse, N. J., Goldstein, J. C., von Ahsen, O., Schuller, M., Newmeyer, D. D., and Green, D. R. (1999) Cytochrome *c* maintains mitochondrial transmembrane potential and ATP generation after outer mitochondrial membrane permeabilization during the apoptotic process. *J. Cell Biol. 153*, 319−328.

(24) Ricci, J.-E., Gottlieb, R. A., and Green, D. R. (2003) Caspase-mediated loss of mitochondrial function and generation of reactive oxygen species during apoptosis. *J. Cell Biol. 160*, 65−75.

(25) Mizutani, H., Tada-Oikawa, S., Hiraku, Y., Kojima, M., and Kawanishi, S. (2005) Mechanism of apoptosis induced by doxorubicin through the generation of hydrogen peroxide. *Life Sci. 76*, 1439−1453.